Electronic Supplementary Material (ESI) for Physical Chemistry Chemical Physics.

Electronic Supplementary Information (ESI) for PCCP:

On the slowdown mechanism of water dynamics around small amphiphiles

Wagner Homsi Brandeburgo,[a,b] Sietse Thijmen van der Post, [c] Evert Jan Meijer,[a,b] and Bernd Ensing [*a,b]

1 Orientational autocorrelation function fits

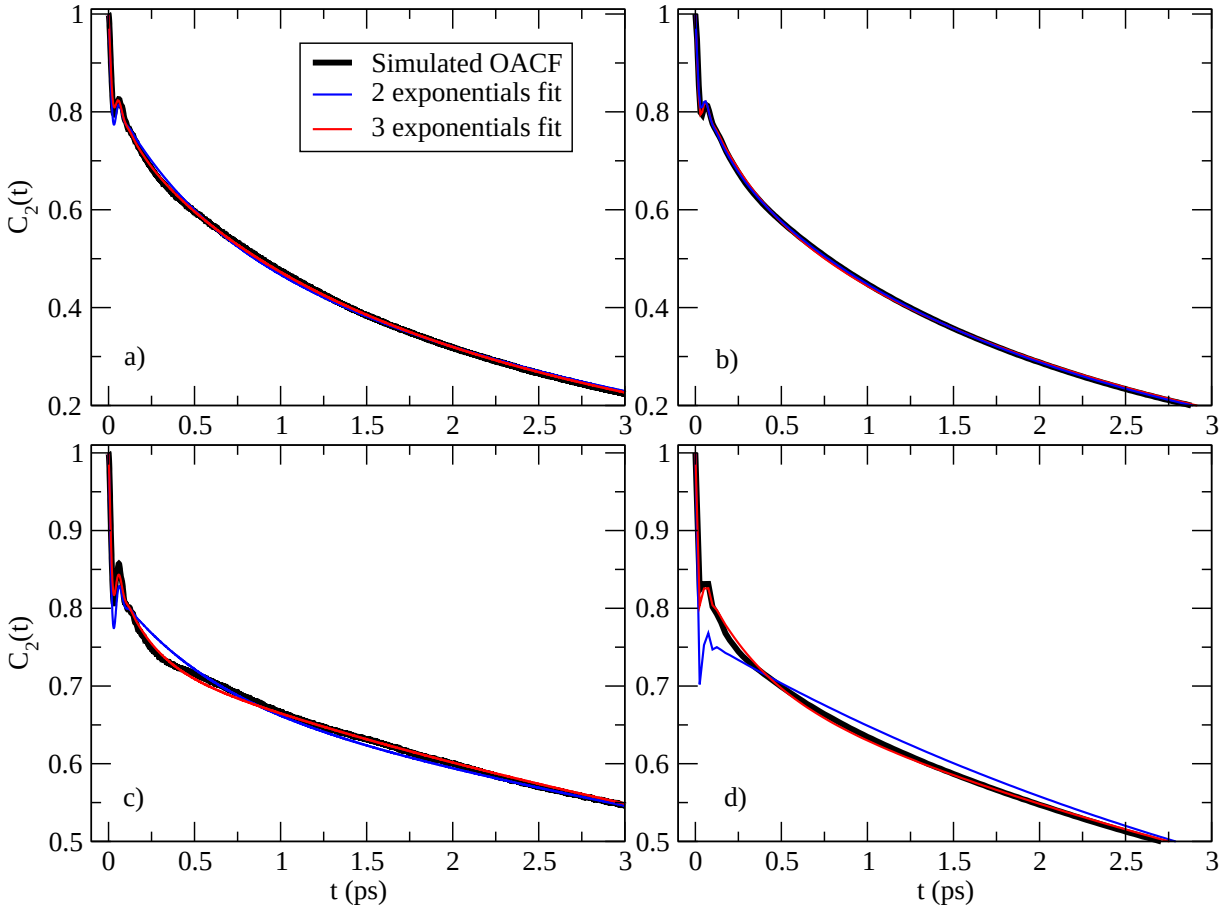

Fig. 1 Comparison between 2 and 3 exponential fits for the OACF of the TMU aqueous systems: upper panels (a and b) are pure water systems; lower panels (c and d) are TMU-water mixture; left panels (a and c) are AIMD simulations; and right panels (b and d) are CMD simulations.

[a] *Van 't Hoff Institute for Molecular Sciences, Universiteit van Amsterdam, Science Park 904, 1098 XH Amsterdam, The Netherlands; E-mail: b.ensing@uva.nl*
[b] *Amsterdam Center for Multiscale Modeling, De Boelelaan 1081a, De Boelelaan 1081a, The Netherlands*
[c] FOM Institute AMOLF, Science Park 104, 1098 XG Amsterdam, The Netherlands

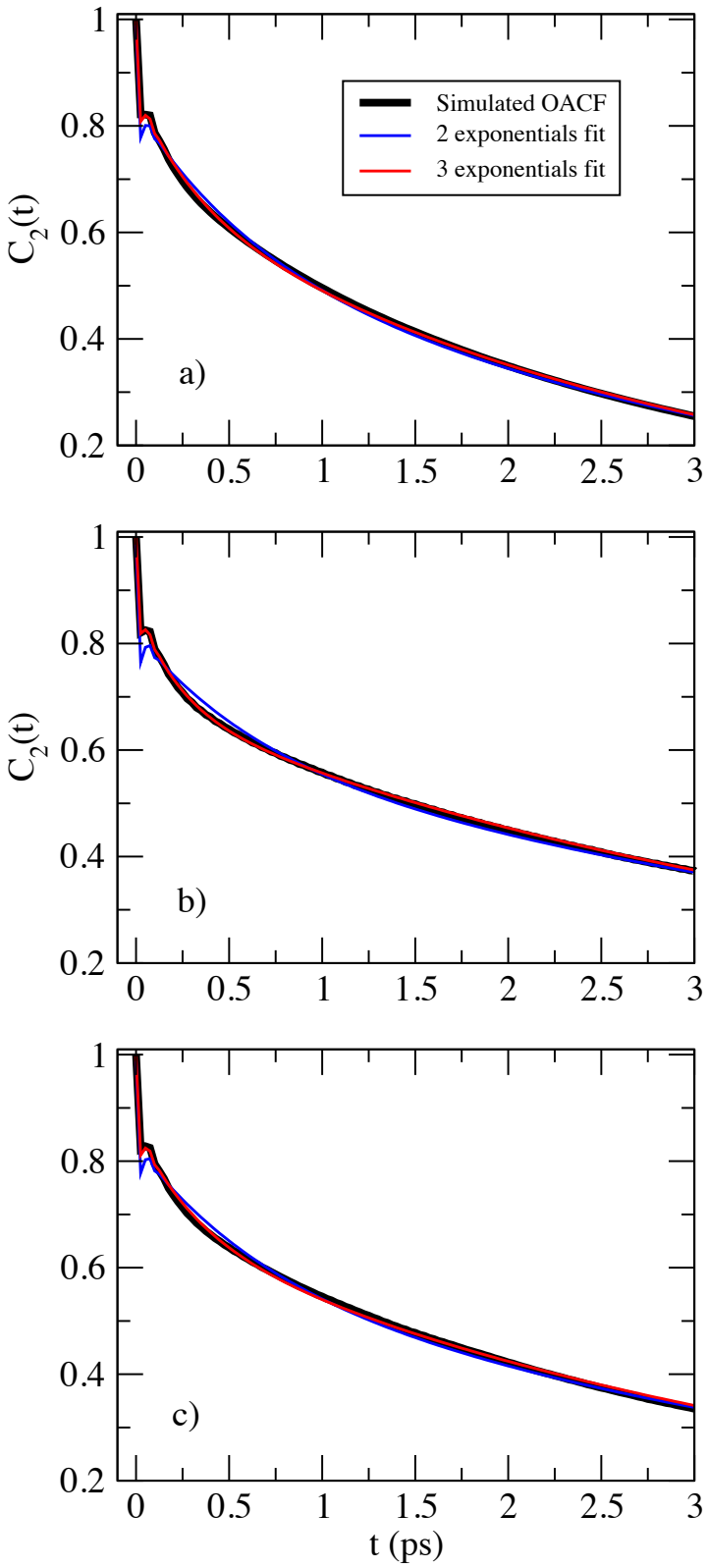

Fig. 2 Comparison between 2 and 3 exponential fits for the OACF of the urea aqueous system: panel 'a' is all water; panel 'b' is the hydrophilic water; and panel 'c' is the hydrophobic water.

Table 1 Relaxation times obtained from the OACF of the aqueous urea system with a 3 exponential fit, since there is a wide range of possible values for the relaxation times yielding a similar quality we fixed τ_{mid} to match the H-bond lifetime for each water type.

System method	Fit interval(ps)	τ_{fast}(ps)	τ_{mid}(ps)	τ_{slow}(ps)
Urea CMD	0 - 20			
All water		0.4	2.6	5.5
Hydrophilic water		0.2	3.1	8.7
Hydrophobic water		0.3	2.7	6.7

2 CMD survival function

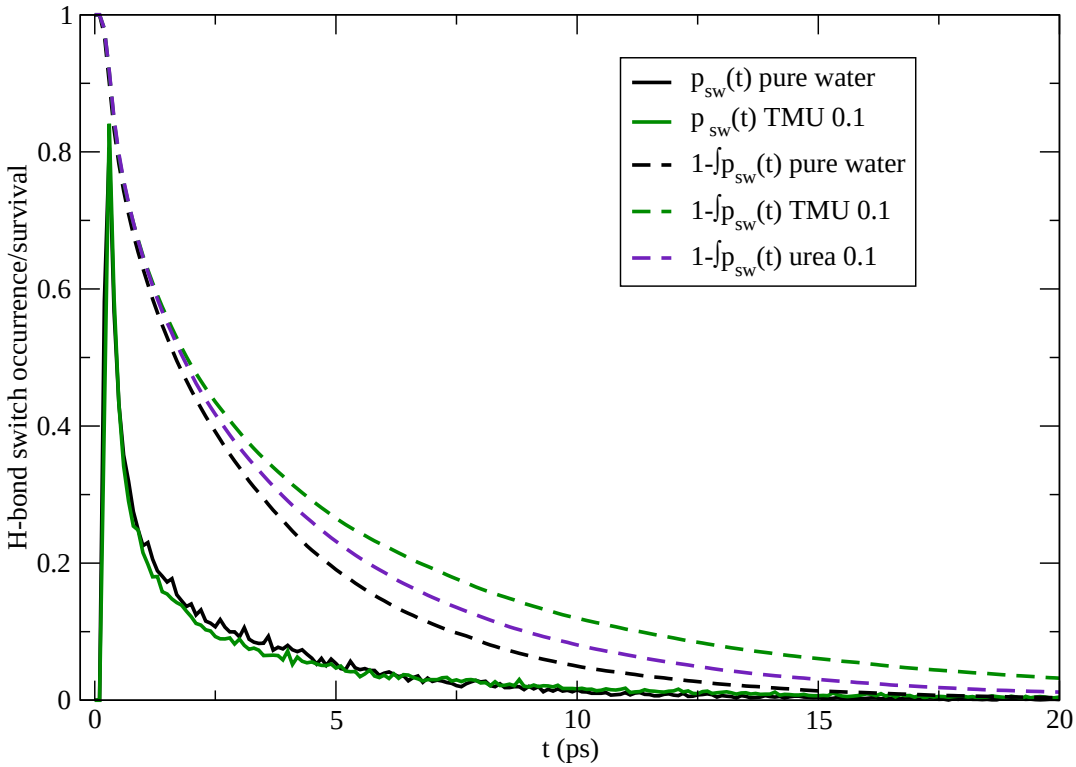

Fig. 3 H-bond switch probability density, $p_{sw}(t)$ (solid lines), and survival function, $1-\int p_{sw}(t)$ (dashed lines), obtained from the CMD simulations. Black lines are for pure water, green lines for the TMU solution and the violet line is for the urea solution. The urea switch function is between TMU and urea and it is omitted here for visualization clarity.

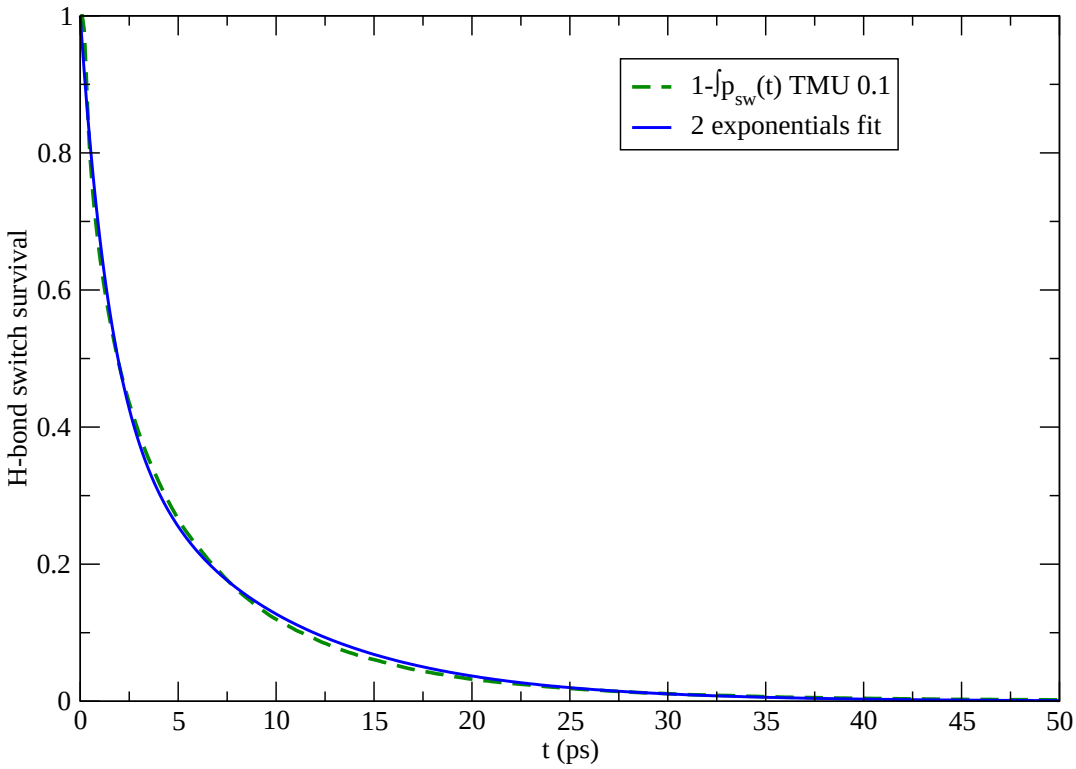

Fig. 4 Survival function (dashed green line) and biexponential fit (solid blue line) for the TMU CMD w=0.1 system.

The Survival function for the TMU CMD system was fitted to a biexponental function with relaxation times: τ_1=1.5 ps, and τ_2=8.1 ps.

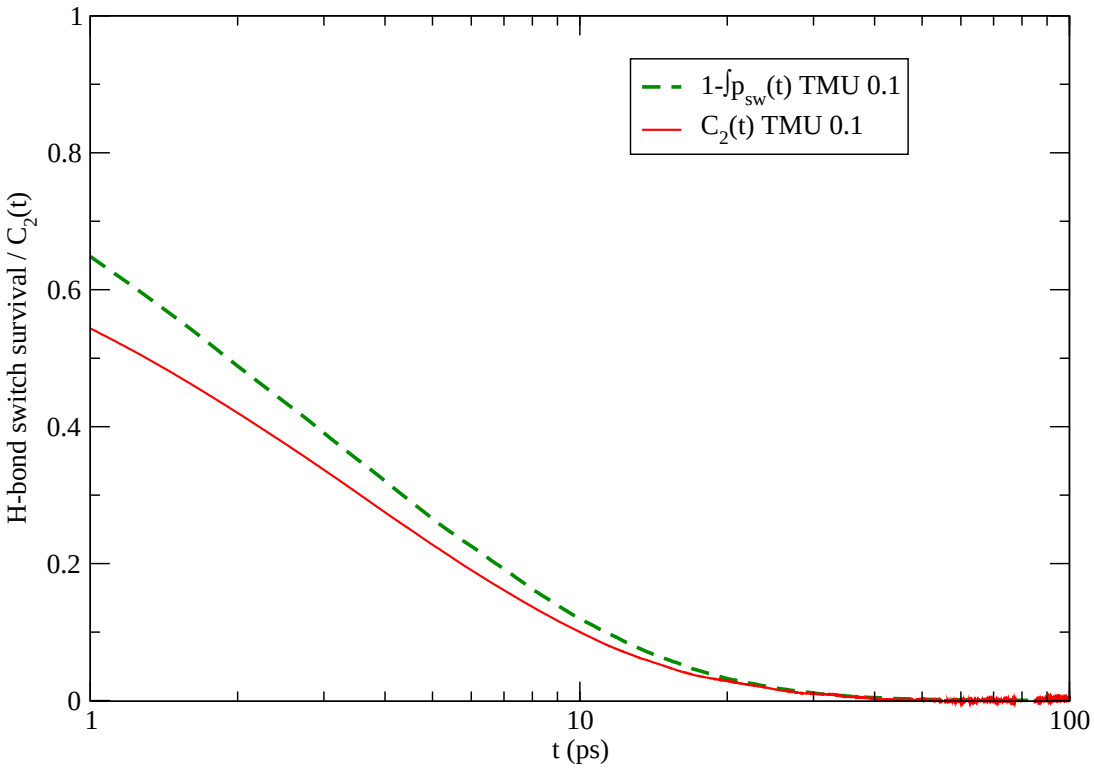

Fig. 5 The OACF and the survival function for the aqueous TMU system simulated with CMD. Note how the slow decaying tails match for both functions at longer times.

3 Vibrational Spectrum

In order to compare the frequency range of water molecules that are H-bonded to a TMU with water molecules that are H-bonded to other water molecules, we calculated the nuclear vibrational frequencies ω from the Fourier transform of the velocity **v(t)** autocorrelation function from selected atoms i in the AIMD simulations. The autocorrelation function was symmetrized at t=0.

$$Q_{vib}(\omega) = \sum_{i=1,N} \int_{-\tau_{max}}^{+\tau_{max}} \langle \mathbf{v}_i(0) \cdot \mathbf{v}_i(t) \rangle \, e^{iwt} \mathrm{d}t \tag{1}$$

For such we have used the H-bond criteria (as described in the first section in results) plus a time buffer of 200 fs for H-bond breaking, however, no time buffer was required for the formation of such bonds. After establishing which water molecules were donating H-bonds, we selected the water hydrogens that participated in those bonds. Therefore, τ_{max} is limited by the H-bond lifetime, an additional smoothing function with an exponential decay was also used for the autocorrelation function.

4 AIMD Orientational Autocorrelation Error

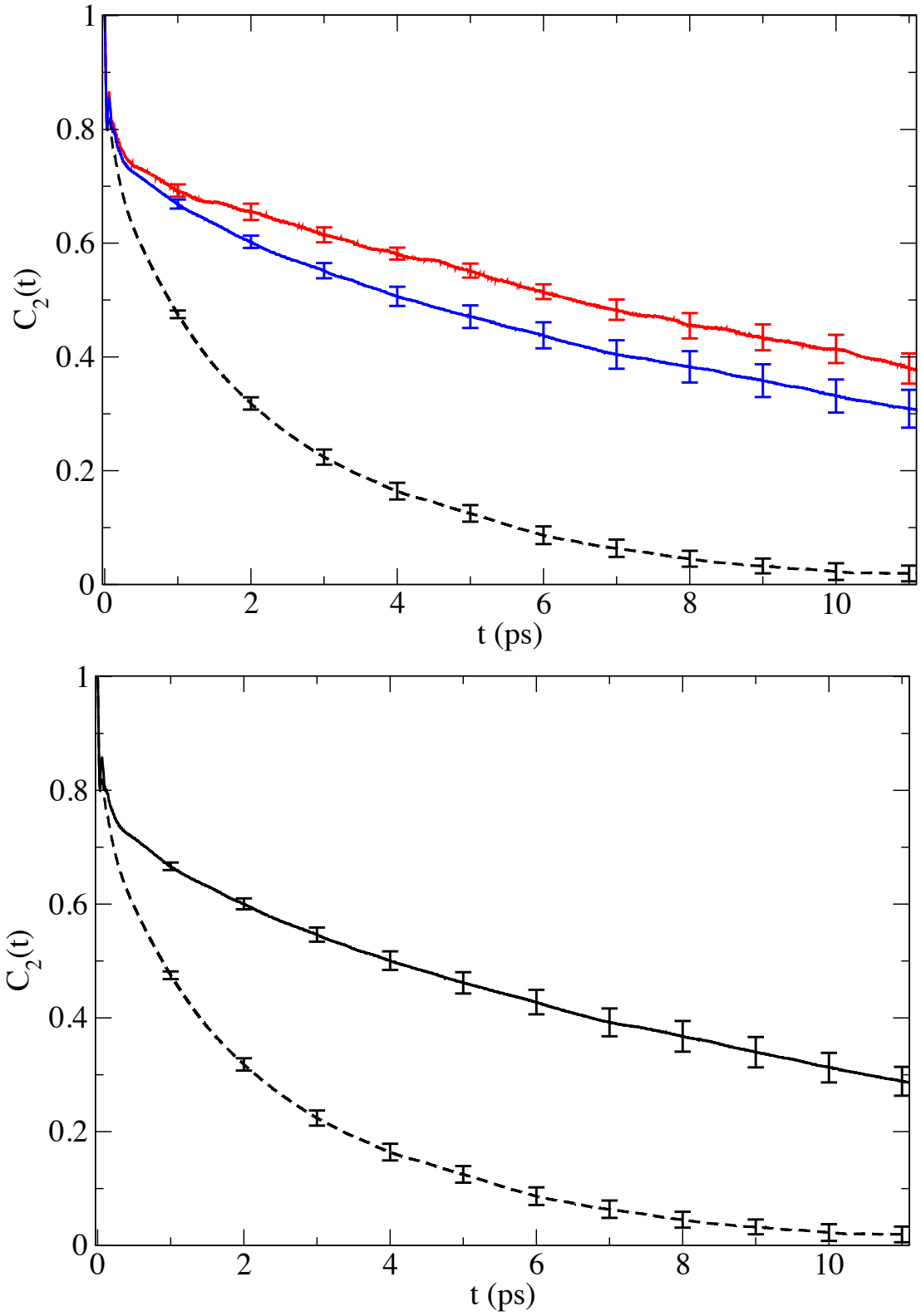

Fig. 6 Simulated water OACF for the different water types from AIMD in TMU solution with error bars. The labels follow the color scheme from Figure 4 with blue for non-hydrophilic, red for hydrophilic and orange for bulk-like water. The solid black line is the solution's total anisotropy and the dashed line is from the pure water system.

5 Energy conservation in AIMD

The energy conservation (Figure 7) throughout the trajectory of the water system. There is a minor divergence of roughly 0.0005 Hartree which is too small to have any significant impact in the dynamics. Nevertheless, we relate this divergence to small numerical errors in CP2K, thermostat, SCF cycle convergence criteria and timestep size. Even though a timestep of 0.5 fs should be enough to cover the fastest water modes; such as the OH stretch which has a period of 10 fs in average.

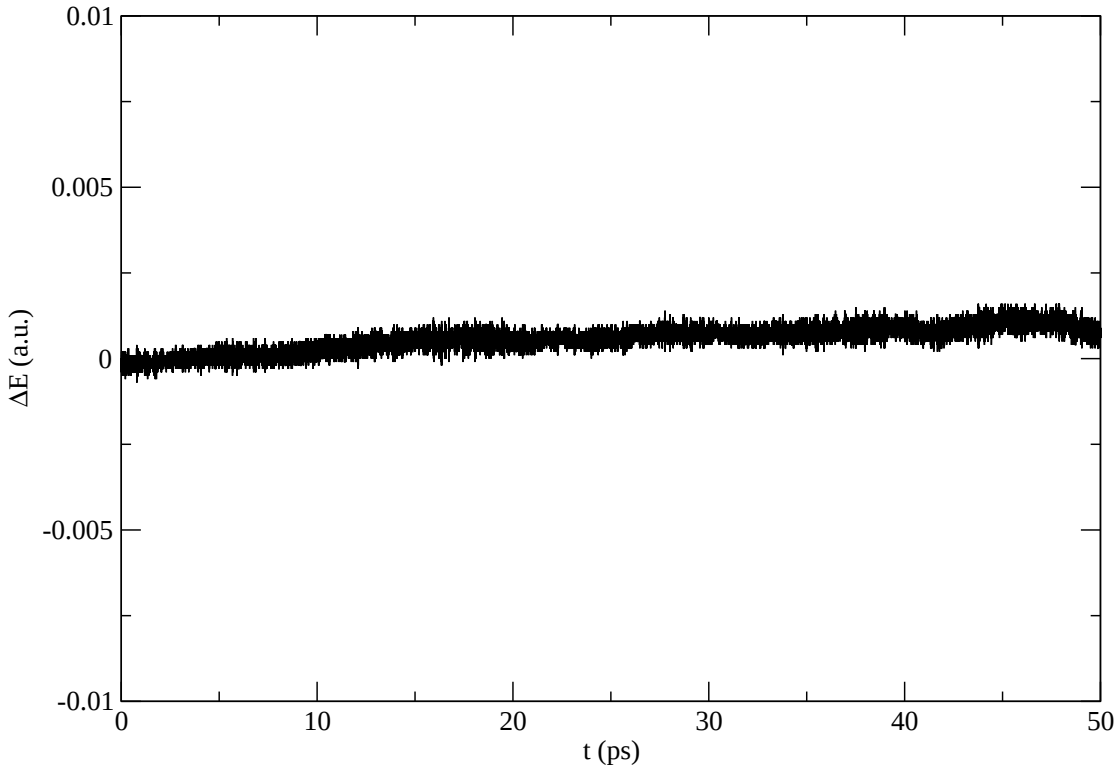

Fig. 7 Variation of the total energy during the water simulation, the first point was used as reference.

6 Mid-Infrared Pump Probe

Polarization resolved fs-IR enables us to experimentally obtain the second order correlation function $C_2(t)$ of the transition dipole moments of the OD stretch vibration in isotopically diluted water (8% HDO molecules in H_2O). To this end we use a probe pulse to measure the absorption change in a sample due to the excitation of the OD stretch vibrational mode by an intense pump pulse. The difference, between the transmission spectra with ($I(\nu,t)$) and without ($I_0(\nu)$) a preceding pump-excitation, is called a transient spectrum $\Delta\alpha(\nu,t)$ and can be written in terms of the measured intensities as,

$$\Delta\alpha(\nu,t) = -\ln\left(\frac{I(\nu,t)}{I_0(\nu)}\right) \tag{2}$$

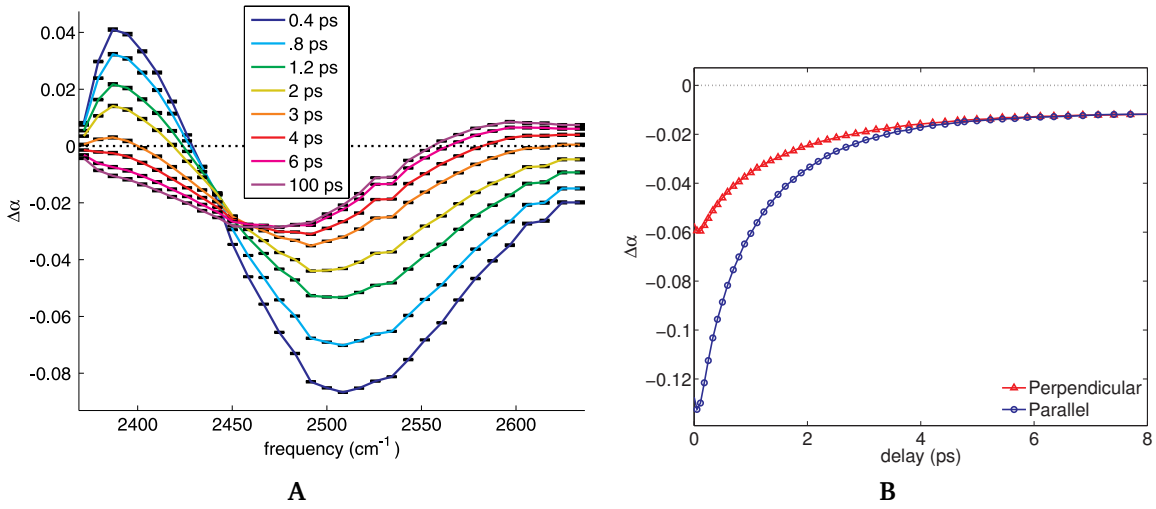

Fig. 8 (**A**) The transient spectra for various pump-probe delay times obtained with the probe polarization parallel to the pump polarization. The sample used is 8% HDO in H_2O. (**B**) The transient absorption difference probed at 2500 cm^{-1} with a probe pulse polarized parallel (circles) and perpendicularly (triangles) to the pump polarization. The parallel signal is initially larger due to the anisotropic excitation. After a few picoseconds both signals become identical due to molecular reorientation.

where ν denotes the frequency and t the delay time between the pump and the probe pulses. Typically, the transmission spectra I are normalized to the spectrum of a reference pulse that is not overlapping with the pump pulse, in order to divide out intensity fluctuations of the laser.

For a number of pump-probe delay times $\Delta\alpha(\nu,t)$ is plotted in Fig. 8A. The transient spectra at short delay times contain three main contributions. First, the pump excites the OD stretch mode of a small percentage of the HDO molecules to their first excited state $|\nu_s{=}1\rangle$. Due to the decreased population in the ground state, the excitation results in a reduced absorption at the $\nu_s = 0 \rightarrow 1$ transition frequency of this mode. The reduced absorption ($\Delta\alpha(\nu,t)$ is negative) is called the ground state bleach. Second, stimulated emission out of the $|\nu_s{=}1\rangle$ state occurs and contributes to the absorption decrease at the $\nu_s = 0 \rightarrow 1$ transition frequency. Finally, the absorption of the probe pulse due to the $\nu_s = 1 \rightarrow 2$ excitation of pump-excited modes leads to an induced absorption ($\Delta\alpha(\nu,t)$ is positive). Since the OD stretch vibrational mode is anharmonic, the spectrum associated with the $\nu_s = 1 \rightarrow 2$ transition is red-shifted by $\sim$180 cm^{-1} from the $\nu_s = 0 \rightarrow 1$. By increasing the pump-probe delay, an increasing number of excited HDO molecules have relaxed to their ground state, causing all three contributions to the transient spectra to decrease in amplitude. Time resolved transient spectra $\Delta\alpha(\nu,t)$ thus contain information on the decay of the probed vibrational mode.

In case the excitation pulse was linearly polarized, the measured response depends on the polarization of the probe pulse. Since the excitation probability scales with $\cos^2(\alpha)$, where α is the angle between the excitation polarization and the transition dipole moment of the vibrational mode, mostly OD groups oriented parallel to the pump polarization will get excited. Immediately after excitation, changes in the absorption that are probed parallel to the pump polarization will therefore be larger than those probed perpendicular to the pump polarization. After a certain delay time the OD stretch modes will be less ordered due to molecular reorientation. As a consequence, the absorption changes will show less dependency on the direction of the probe polarization, i.e. exhibit a more isotropic behavior. An example of the parallel and perpendicular absorption changes probed in 8% HDO in H_2O at 2500 cm^{-1} for different delay times is shown in Fig. 8B. The dynamical behavior of such a polarization resolved experiment thus not only depends on the vibrational decay of the excited mode, but on the reorientation dynamics as well. A parameter that exclusively depends on the reorientation of the excited transition dipole moments is the anisotropy $R(\nu,t)$ given by,

$$R(\nu,t) = \frac{\Delta\alpha_{\parallel}(\nu,t) - \Delta\alpha_{\perp}(\nu,t)}{\Delta\alpha_{\parallel}(\nu,t) + 2\Delta\alpha_{\perp}(\nu,t)} \tag{3}$$

The dynamic behavior of $R(\nu,t)$ is equal to that of the second order dipole-dipole correlation function and differs in

amplitude by a factor of 2/5.

7 Modeling Heat Dynamics

It should be noted that the signals in Fig. 8B do not decay completely but rather reach an endlevel after ~ 10 ps. This response at long delay times is not due to excited OD oscillators and should be subtracted from the data before calculating the anisotropy. The response is found to grow on a similar timescale as the decay of the excitation[1] and to remain constant for longer delay times, at least on the timescale of the experiment (100 ps). The origin of this contribution is the rise in temperature of the sample due to dissipation of the vibrational energy into thermal bath modes. As a response to the new energy content, the hydrogen-bonds in the solution will weaken. OD-oscillators with a weaker hydrogen-bond have a lower cross section and their resonance frequency is shifted towards blue frequencies. This explains the spectral shape of the thermal endlevel found in our experiments for long pump-probe delays: a bleach at red frequencies and a much smaller induced absorption a blue frequencies (Fig. 8A). To be able to subtract this spectral weight also at short delays we need to know its dynamics. To that end we measured the thermal response at the red shoulder of the OH-stretch vibration around 3000 cm^{-1} after excitation of the OD stretch vibration. This spectral window is free from the transient response of the OD oscillators. This method was elaborated on a previous work[1]. The thermalization dynamics thus obtained is used to subtract the heat component from a pump-probe measurement on the OD stretch vibration by first fitting a multi-exponential function to the thermalization curve to capture the dynamics $N_H(t)$. No assumptions are made on the fit based on physical interpretation, since it merely serves the purpose of describing the measured dynamics. Typically, a function of three exponentials was found to accurately describe the curves. For the thermal difference spectrum $\sigma_H(\nu)$, the transient spectrum at long delay time is used of the dataset of which the thermal contribution is to be subtracted. For improved signal-to-noise, we took the average transient spectrum of at least three delay times between 70 and 100 ps. Having obtained a description of $N_H(t)$ and $\sigma_H(\nu)$, finally the heat subtracted transient spectra are given by,

$$\widetilde{\Delta\alpha}_{\parallel}(\nu,t) = \Delta\alpha_{\parallel}(\nu,t) - N_H(t)\sigma_H(\nu) \tag{4}$$

$$\widetilde{\Delta\alpha}_{\perp}(\nu,t) = \Delta\alpha_{\perp}(\nu,t) - N_H(t)\sigma_H(\nu) \tag{5}$$

8 Experimental Setup

As the reorientation timescale is in the order of picoseconds, the measurements require a sub-picosecond pump and probe pulse duration. The laser system used to generate these pulses is a regenerative Ti:Sapphire laser (Coherent), providing pulses at 800 nm with a duration of 35 fs and a pulse energy of 3.5 mJ at a repetition rate of 1 kHz. Since the resonance frequency of the OD strech mode in HDO molecules is 2500 cm^{-1}, these pulses need to be downconverted. To this end, the output of the laser is split in three portions of interest: (1) 850 μJ to pump a homebuilt optical parametric amplifier (OPA) to generate the probe light, (2) 850 μJ to pump a TOPAS (LightConversion) and (3) 1.3 mJ to pump a difference frequency mixing stage after the TOPAS to generate mid-IR pulses that are used as pump. The pump pulses are generated by pumping a TOPAS (LightConversion) based on super-fluorescence. The TOPAS down-converts the pulses in a β-Borium-Borate (BBO) crystal to signal (p-polarized) and idler (s-polarized) pulses of 1333 nm and 2000 nm with a total energy of 280μJ. The idler pulses are doubled in a 1 mm BBO crystal to create 1 μm pulses, which are finally difference frequency mixed with the 1.3 mJ portion of 800 nm light out of the Ti-Sapphire laser. This last conversion step yields light pulses with a central frequency of 2500 cm^{-1} (using $LiNbO_3$ as DFG crystal). The spectral bandwidth is 150 cm^{-1} and pulse energy 50 μJ.

The homebuild OPA is built according to the geometry developed by the group of Peter Hamm. The OPA is white-light seeded and generates a signal and idler pulse in a parametric amplification process in a BBO crystal (2 mm). The signal and idler are difference frequency mixed in a silver-gallium-disulfide crystal (1.2 mm), yielding mid-IR pulses of which the frequency was tuned to 2500 cm^{-1}. At this frequency, the pulse energy is 5 μJ, the FWHM of the pulse spectra is 300 cm^{-1}. The generated pulses are s-polarized. Only 8 percent of this light was used as the probe light, split of by a ZnSe beamsplitter wedge. The cross-correlate between the pump and probe pulses as obtained in a thin germanium window is 150 fs, mainly determined by the pump pulse duration.

Probe pulses are sent into a variable delay stage with a time-resolution of 6.6 fs. With the delay stage we vary the time delay t between pump and probe. The reflection from the back side of the wedged ZnSe plate serves as a reference

pulse. The pump is transmitted through a $\lambda/2$ plate to rotate its polarization at 45 degrees with respect to that of the probe. The pump, probe and reference are all focused in the sample using a gold-coated parabolic mirror, but only the pump and the probe are in spatial overlap. After the sample, a mechanically rotated polarizer selects the polarization component of the probe pulse either parallel or perpendicular to the pump polarization. After recollimation of the beams with a second parabolic mirror, the probe and the reference are dispersed with an Oriel monochromator and detected on two separate lines of an Infrared Associates 3×32 mercury-cadmium-telluride (MCT) detector array. The measurement of the reference thus allows for a frequency-resolved correction for shot-to-shot fluctuations of the probe-pulse energy.

Âğhe sample is contained in between two CaF_2 windows of 0.5 mm thickness, separated by a teflon spacer of 25 μ m thickness. We used millipore water and added 4 vol.% D_2O (Sigma Aldrich, 99.9% purity) to get isotopically diluted water. TMU (Sigma Aldrich) was added to obtain a 6 molal solution.

References

1 S. T. van der Post and H. J. Bakker, *J. Phys. Chem. B*, 2014, **118**, 8179–8189.